ELSEVIER

Journal of Molecular Catalysis A: Chemical 162 (2000) 287–295

JOURNAL OF MOLECULAR CATALYSIS A: CHEMICAL

www.elsevier.com/locate/molcata

Distinguishing surface and bulk electron charge carriers for ZnO powders

A.B. Walters *, B.-K. Na, C.-C. Liu, M.A. Vannice

Department of Chemical Engineering, The Pennsylvania State University, 158 Fenske Laboratory, University Park, PA 16802, USA

Abstract

A two-charge-carrier model that assumes coexisting high-mobility, low-concentration bulk, semiconduction electron charge carriers and low-mobility, variable-concentration surface-trapped-electron charge carriers is used to explain measured electrical and chemisorption properties of ZnO powders. This model resolves two serious quantitative issues not explained by the single-charge-carrier-type model used for our previously reported studies. Not explainable using a single-charge-carrier model are (1) wide variations in measured electron mobility values due to variations in surface treatments and (2) calculated electron number densities too low to match measured electron-transfer chemisorption results. Our two-charge-carrier model for ZnO powders assigns high-mobility bulk electrons to n-type ZnO semiconduction and low-mobility surface electrons to $(V_o)^{2-}$ and $(V_o^+)^-$ surface oxide ion electron trapping vacancies. This model results in a high variation in surface electron number density due to surface treatments, while the mobilities for both the bulk and surface charge carriers remain constant. The model also calculates much higher surface electron number densities that better match charge-transfer chemisorption results. The two-charge-carrier model is expected to have significant importance in explaining chemisorption and catalysis on ZnO and other similar powder oxides. In particular, the two-charge-carrier model can yield two to three orders of magnitude higher calculated concentrations of surface electrons than for the single-charge-carrier model for any powder with coexisting high-mobility, semiconduction, bulk charge carriers and variable concentrations of low-mobility, surface charge carriers. © 2000 Published by Elsevier Science B.V.

Keywords: Electron charge carriers; ZnO powders; Two-charge-carrier model

1. Introduction

Correlations between changes in electrical conductivity and other measured changes at the surfaces of high-surface-area solids are often used to describe electrical charge-carrier-related chemistry at solid surfaces. However, without charge carrier mobility measurements, changes in the actual number densities of charge carriers cannot be quantitatively correlated with chemisorption, IR, ESR, or other quantitative measurements of chemistry changes at solid surfaces.

Previously reported studies of ZnO powder electrical properties from our laboratory [1–5] employed a microwave Hall effect (MHE) system to measure both electrical mobility and conductivity so that the number densities of charge carriers could be quantitatively determined and correlated to chemisorption, ESR, and IR measurements of changes at ZnO surfaces. We used a single-electron-type-charge-carrier

* Corresponding author.

1381-1169/00/$ - see front matter © 2000 Published by Elsevier Science B.V.
PII: S1381-1169(00)00297-1

model to explain our results. The use of this model left unresolved the following two distinct quantitative issues, (a) our measured electron mobilities, μ ($cm^2/V \cdot s$), were highly variable, depending on surface treatments, and, in many cases, much lower than mobilities previously reported for ZnO, and (b) the concentrations of charge-transfer, chemisorbed species determined by ESR and chemisorption measurements were often much higher than the measured concentrations of available surface electrons, n_S (electrons/cm^3) or N_S (electrons/g), calculated from our measured conductivities and mobilities.

Both of these issues can be resolved by using a two-electron charge carrier model. This model is consistent with the assumptions that the low number densities of high-mobility bulk semiconduction electron charge carriers are not significantly affected by surface treatments and that the number densities of low-mobility electrons trapped at surface $(V_o)^{2-}$ and $(V_o^+)^-$ centers vary widely depending on surface treatments. In addition, we are able to reasonably fit all of our electrical property data using a single mobility value, μ_B, of 200 $cm^2/V \cdot s$ for the bulk semiconduction electrons and a single mobility, μ_S, of 0.1 $cm^2/V \cdot s$ for the surface $(V_o)^{2-}$ and $(V_o^+)^-$ trapped electrons. The bulk ZnO μ_B value selected is at the high end of the values (90 to 200 $cm^2/V \cdot s$) previously reported for bulk ZnO (Table 3, Ref. [2]), and the selected μ_S value of 0.1 $cm^2/V \cdot s$ for surface electrons is at the high end of the values (range of 0.001 to 0.1 $cm^2/V \cdot s$) determined for ZnO nanoparticles [7] and is also consistent with the μ_S value required to produce reasonable calculated N_B values and quantitative agreement with charge-transfer chemisorbed species.

2. Experimental

As in our previously published studies of ZnO powders [1–5], electric charge carrier mobility and conductivity are measured by microwave techniques, ESR is used to study both solid surface defect chemistry and ESR-active chemisorbed gases, and standard chemisorption measurements are used to quantify gas chemisorptions and specific surface areas.

A new high purity ZnO powder was prepared by adding a 1 M $(NH_4)_2CO_3$ (Aesar, 99.999%) solution drop by drop to a $Zn(NO_3)_2$ (Aldrich, 99.999%) solution while stirring to precipitate $ZnCO_3$. The precipitate was washed thoroughly with distilled, deionized water to remove residue NH_4^+ ions, filtered, and oven dried at 393 K for 48 h, then stored in a desiccator. The $ZnCO_3$ was decomposed to ZnO inside a quartz cell by heating under vacuum ($< 1 \times 10^{-6}$ Torr) at a rate of 2 K/min to 403 K, holding for 1 h at 403 K, heating to 533 K at 2 K/min, holding for 30 min at 533 K, then heating to 673 K, again at a rate of 2 K/min, and holding for 30 min at 673 K for 4 h. The slow heating rate facilitated the retention of high surface area when decomposing $ZnCO_3$ to ZnO. The measured surface area of the new ZnO powder was initially 27.7 m^2/g, and gradually decreased to 20.1 m^2/g after the completion of surface treatment cycles.

ESR experiments were carried out with a commercial IBM (Bruker) ER 200D spectrometer equipped with a standard TE102 rectangular cavity and variable temperature unit (ER 4111VT) with a measurement temperature range from 100 to 573 K. The g-values and spin concentrations were determined by comparison to both a weak pitch standard (Bruker, $g = 2.0028$) and a sample composed of three parts DPPH powder (Sigma, $g = 2.0037$) diluted with 1000 parts pre-calcined ultra-high-purity SiO_2 powder (Davidson 57). Typically, microwave power levels of 2–5 mW and a modulation amplitude of 1.0 G were used during measurements. Spin concentrations were calculated by computer double integration of the first derivative spectrum of the ESR signal using digitized data. ESR sample tubes were constructed from 4.0-mm o.d. quartz tubing (Wilmad 707-SQ) with a high-vacuum valve (Ace glass, 8195-45) to allow evacuation and in-situ adsorption of gases. The quartz tube was filled with a powder sample over a length of approximately 7 to 8 cm, considerably longer than the effective cavity length of about 2 cm, to avoid any quantitative errors due to an inadvertent change in the position of the sample tube inside the cavity. These tubes were attached to a UHV gas handling system [6].

Microwave conductivity and mobility experiments were carried out using the IBM (Bruker) ER 200D ESR spectrometer equipped with a custom, rectangu-

lar TE102 bimodal resonant cavity using modifications described in our previously published descriptions of the experimental apparatus for conductivity and mobility measurements [1–6]. A new 5-mm o.d. quartz tube (Wilmad 703-PQ) and a new high-vacuum valve (Ace Glass, 8195-45) were used for microwave electrical property measurements. Absolute values for Hall mobility, μ ($cm^2/V \cdot s$), and electrical conductivity, σ ($(\Omega\ cm)^{-1}$) were calculated using equations presented in our earlier publications for the low-conductivity region [2–5].

3. Results

The results for our previous and new electrical property measurements for ZnO powders are presented in Tables 1–6. The values for calculated charge carrier concentrations, N_C (electrons/g $\times 10^{-15}$), using the single-charge-carrier model, are presented in the first three columns along with the measured values for conductivity, σ_{meas} ($(\Omega\ cm)^{-1} \times 10^3$) and mobility μ_{meas} ($cm^2/V \cdot s$). The calculated values for the bulk electron densities, N_B (electrons/g $\times 10^{-15}$), and surface electron densities, N_S (electrons/g $\times 10^{-15}$) using the two-charge-carrier model are presented in the last two columns of Tables 1–6. As can be seen, the two-charge-carrier model N_S values can be two to three orders of magnitude higher than for the N_C values calculated using the single charge-carrier-model. Also shown is the effect of specific surface area on the values for N_B and N_S. ZnO(I) has about 10 times the calculated N_S values compared to those for the 10 times lower

Table 1
ZnO(I) ($\cong$ 27–32 m^2/g) electrical properties at 298 K (Refs. [1,2])

Treatment	Meas. $\sigma \times 10^3$	Meas. μ	Calc. $N_C \times 10^{-15}$	Calc. $N_B \times 10^{-15}$	Calc. $N_S \times 10^{-15}$
673 K evac., 4 h	1.20	3.9	0.343	0.000127	13.109
20 Torr O_2	0.50	20.0	0.028	0.000277	5.014
673 K evac., 2 h	62.00	2.5	27.617	0.004145	682.134
20 Torr O_2	1.00	67.0	0.017	0.001863	7.409
300 K evac., 1 h	1.50	42.0	0.040	0.001751	13.203
673 K evac., 2 h	68.00	2.5	30.290	0.004546	748.147
2.0 Torr CO	56.00	2.5	24.944	0.003744	616.121
20 Torr CO	61.00	2.5	27.171	0.004078	671.132
300 K evac. 1 h 20 torr O_2	1.80	19.0	0.105	0.000948	18.149
673 K evac., 2 h	61.00	2.5	27.171	0.004078	671.132
2.0 Torr O_2	2.40	36.0	0.074	0.002400	21.926
20 Torr O_2	1.60	55.0	0.032	0.002447	12.924
300 K evac., 1 h	2.10	21.0	0.111	0.001222	20.940
2.0 Torr CO	12.00	2.7	4.949	0.000869	131.892
20 Torr CO	21.00	2.6	8.994	0.001462	230.928
673 K evac., 2 h	46.00	2.5	20.490	0.003075	506.099
2.0 Torr H_2	40.00	2.5	17.817	0.002674	440.086
20 Torr H_2	38.00	2.5	16.927	0.002540	418.082
300 K evac., 1 h, 20 torr O_2	2.20	13.0	0.188	0.000790	22.918
673 K evac., 2 h	50.00	2.5	22.272	0.003342	550.108
20 Torr O_2	1.30	18.0	0.080	0.000648	13.180
300 K evac., 1 h, 20 Torr H_2	1.60	16.0	0.111	0.000709	16.400
673 K evac. 2 h	62.00	3.4	20.307	0.005699	679.025
20 Torr CO_2	7.50	5.7	1.465	0.001170	81.179
673 K evac., 2 h	70.00	3.4	22.927	0.006434	766.642
20 Torr O_2 evac., 1 h, 300 K	3.60	6.5	0.617	0.000642	38.806
20 Torr CO_2	1.60	11.0	0.162	0.000486	16.846
673 K evac., 2 h, 200 Torr O_2	0.60	46.0	0.015	0.000767	5.147

(N_B and N_S calculated for $\mu_B = 200\ cm^2/V \cdot s$ and $\mu_S = 0.1\ cm^2/V \cdot s$).

Table 2
ZnO(I) ($\cong$ 27–32 m^2/g) electrical properties at 298 K (Refs. [1,2])

Treatment	Meas. $\sigma \times 10^3$	Meas. μ	Calc. $N_C \times 10^{-15}$	Calc. $N_B \times 10^{-15}$	Calc. $N_S \times 10^{-15}$
673 K evac., 4 h	6.40	4.4	1.620	0.000767	69.736
20 Torr O_2	0.56	59.0	0.011	0.000919	4.399
673 K evac., 1 h	24.00	4.6	5.810	0.003008	261.244
20 Torr O_2	0.85	31.0	0.031	0.000732	8.002
300 K evac., 0.5 h	0.84	27.0	0.035	0.000629	8.095
673 K, 2 h, 200 Torr O_2	0.19	42.0	0.005	0.000222	1.672
473 K evac., 2 h	3.00	5.7	0.586	0.000468	32.472
20 Torr O_2	1.00	10.0	0.111	0.000276	10.584
473 K evac., 3 h	6.90	8.0	0.960	0.001518	73.801
20 Torr O_2	1.50	26.0	0.064	0.001082	14.540
473 K evac., 5 h	8.10	11.0	0.820	0.002459	85.282
20 Torr O_2	1.50	16.0	0.104	0.000664	15.375
673 K evac., 2 h	75.00	4.2	19.885	0.008565	818.059
20 Torr O_2	4.90	7.0	0.780	0.000942	52.682
300 K evac., 1 h	5.60	6.7	0.931	0.001029	60.302

(N_B and N_S calculated for $\mu_B = 200\ cm^2/V \cdot s$ and $\mu_S = 0.1\ cm^2/V \cdot s$).

specific surface area ZnO(II), while both of these ZnO samples have comparable calculated values for N_B.

3.1. Two-charge-carrier model

The one-charge-carrier model uses the relationship

$$\sigma_{meas} = n_C |e|\, \mu_{meas} \quad (1)$$

where n_C is the charge carrier density in electrons/cm^3, to calculate electron densities in electrons/g using the bulk density of ZnO to convert from electrons/cm^3 to electrons/g. For a single charge carrier, the two independent measurements for σ and μ are adequate to calculate values for n_C or N_C as there is one equation to find the one unknown.

The two-charge-carrier model uses the relationships

$$\sigma_{meas} = n_B |e|\, \mu_B + n_S |e|\, \mu_S \quad (2)$$

for any combination of positive or negative charge carriers,

$$\mu_{meas} = \sigma_{meas} |1/e| \left[\left(n_B\, \mu_B^2 + n_S\, \mu_S^2 \right) / \left(n_B\, \mu_B + n_S\, \mu_S \right)^2 \right] \quad (3)$$

Table 3
ZnO(II) ($\cong$ 3.4 m^2/g) electrical properties at 298 K (Refs. [1,2])

Treatment	Meas. $\sigma \times 10^3$	Meas. μ	Calc. $N_C \times 10^{-15}$	Calc. $N_B \times 10^{-15}$	Calc. $N_S \times 10^{-15}$
673 K evac., 2 h	1.50	4.6	0.363	0.000188	16.328
20 Torr O_2	1.10	9.4	0.130	0.000285	11.680
673 K evac., 2 h	2.10	4.0	0.585	0.000228	22.929
20 Torr O_2	1.20	15.0	0.089	0.000498	12.367
673 K, 2 h, 200 Torr O_2	1.20	19.0	0.070	0.000632	12.100
473 K evac., 2 h	1.90	4.2	0.504	0.000217	20.724
20 Torr O_2	1.50	7.4	0.226	0.000305	16.094
473 K evac., 3 h	2.20	5.0	0.490	0.000300	23.898
20 Torr O_2	1.20	19.0	0.070	0.000632	12.100
473 K evac., 3 h	3.80	3.3	1.282	0.000339	41.639
20 Torr O_2	1.50	7.4	0.226	0.000305	16.094

(N_B and N_S calculated for $\mu_B = 200\ cm^2/V \cdot s$ and $\mu_S = 0.1\ cm^2/V \cdot s$).

Table 4
ZnO(II) (≅ 3.4 m^2/g) electrical properties at 298 K (Refs. [1,2])

Treatment	Meas. $\sigma \times 10^3$	Meas. μ	Calc. $N_C \times 10^{-15}$	Calc. $N_B \times 10^{-15}$	Calc. $N_S \times 10^{-15}$
673 K evac., 1 h	2.8	91.0	0.034	0.007089	17.002
673 K, 2 h, 200 Torr O_2	2.5	113.0	0.025	0.007862	12.116
473 K evac., 5 h	11.0	19.0	0.645	0.005791	110.913
After 20 min	7.3	24.0	0.339	0.004860	71.573
50 Torr O_2	2.9	101.0	0.032	0.008150	15.994
300 K evac., 1 h	5.7	34.0	0.187	0.005382	52.710
50 Torr O_2	3.1	93.0	0.037	0.008022	18.478
673 K evac., 1 h	21.0	13.0	1.799	0.007546	218.762
After 4 h	5.4	26.0	0.231	0.003896	52.342
50 Torr O_2	3.2	90.0	0.040	0.008013	19.609
673 K, 1 h, 700 Torr O_2	2.6	125.0	0.023	0.009045	10.863
300 Torr O_2	2.6	114.0	0.025	0.008249	12.456
100 Torr O_2	2.7	110.0	0.027	0.008265	13.537
50 Torr O_2	2.6	118.0	0.025	0.008538	11.877
300 K evac., 1 h	5.6	26.0	0.240	0.004040	54.281
100 Torr O_2	3.7	41.0	0.100	0.004215	32.773
700 Torr O_2	3.2	63.0	0.057	0.005606	24.422
673 K evac., 2 h	3.6	42.0	0.095	0.004201	31.686

(N_B and N_S calculated for $\mu_B = 200\ cm^2/V \cdot s$ and $\mu_S = 0.1\ cm^2/V \cdot s$).

Table 5
ZnO (new) (≅ 20.1–27.7 m^2/g) electrical properties at 298 K (Refs. [4,5])

Treatment	Meas. $\sigma \times 10^3$	Meas. μ	Calc. $N_C \times 10^{-15}$	Calc. $N_B \times 10^{-15}$	Calc. $N_S \times 10^{-15}$
300 K evac., overnight	0.56	63.90	0.010	0.000995	4.246
673 K evac., 4 h	1.23	25.60	0.054	0.000874	11.950
300 K, 20 Torr O_2 in 1 h	0.49	74.10	0.007	0.001010	3.437
673 K evac., 2 h	1.62	15.80	0.114	0.000708	16.623
300 K, 20 Torr O_2 in 1 h	0.93	34.80	0.030	0.000899	8.559
673 K evac., 2 h	91.00	2.88	35.186	0.007046	999.270
300 K, 20 Torr O_2 in 1 h	8.70	22.80	0.425	0.005501	85.880
300 K evac., 30 min	9.00	27.00	0.371	0.006743	86.736
300 K, 20 Torr CO in 1 h and evac.	11.70	7.60	1.714	0.002444	125.401
673 K evac., 2 h	34.30	3.60	10.610	0.003344	375.272
300 K, 20 Torr O_2 in 1 h	4.20	46.50	0.101	0.005428	35.914
300 K evac., 30 min	4.91	38.00	0.144	0.005183	44.311
300 K, 20 Torr CO in 1 h and evac.	9.54	5.84	1.819	0.001525	103.186
673 K evac., 2 h	82.70	5.10	18.058	0.011517	897.901
300 K, 20 Torr O_2 in 1 h and evac.	4.85	43.80	0.123	0.005903	42.202
300 K, 20 Torr CO in 1 h and evac.	9.65	5.83	1.843	0.001540	104.381
403 K red., 100 Torr H_2 and evac.	14.30	4.50	3.539	0.001753	155.738
300 K, 20 Torr O_2 in 1 h and evac.	5.30	18.90	0.312	0.002775	53.469
403 K red., 100 Torr H_2 and evac.	14.10	2.70	5.815	0.001021	154.973
300 K, 20 Torr O_2 in 1 h and evac.	7.20	25.40	0.316	0.005074	70.031
403 K red., 100 Torr H_2 and evac.	13.20	2.70	5.444	0.000956	145.081
300 K, 20 Torr O_2 in 1 h and evac.	5.40	23.80	0.253	0.003565	53.004
300 K, 20 Torr CO in 1 h and evac.	5.80	17.90	0.361	0.002876	58.837
673 K evac., 2 h	85.80	5.10	18.734	0.011949	931.558
300 K, 20 Torr O_2 in 1 h and evac.	12.30	21.90	0.625	0.007469	122.034
300 K, 20 Torr CO in 1 h and evac.	20.60	10.20	2.249	0.005795	217.808

(N_B and N_S calculated for $\mu_B = 200\ cm^2/V \cdot s$ and $\mu_S = 0.1\ cm^2/V \cdot s$).

Table 6
ZnO (new) (≅ 22 m^2/g) Electrical Properties at 298 K (Refs. [4,5])

Treatment	Meas. $\sigma \times 10^3$	Meas. μ	Calc. $N_C \times 10^{-15}$	Calc. $N_B \times 10^{-15}$	Calc. $N_S \times 10^{-15}$
300 K evac., overnight	0.56	63.90	0.010	0.002501	0.124
673 K evac., 4 h	1.23	25.60	0.054	0.002066	0.445
300 K, 20 Torr O_2 in 1 h	0.49	74.10	0.007	0.002551	0.091
673 K evac., 2 h	1.62	15.80	0.114	0.001567	0.643
300 K, 20 Torr O_2 in 1 h	0.93	34.80	0.030	0.002185	0.305
673 K evac., 2 h	91.00	2.88	35.186	0.002515	40.409
300 K, 20 Torr O_2 in 1 h	8.70	22.80	0.425	0.012844	3.233
300 K, evac. 30 min	9.00	27.00	0.371	0.016036	3.207
300 K, 20 Torr CO in 1 h and evac.	11.70	7.60	1.714	0.004339	4.995
673 K, evac. 2 h	34.30	3.60	10.610	0.002744	15.141
300 K, 20 Torr O_2 in 1 h	4.20	46.50	0.101	0.013439	1.199
300 K, evac. 30 min	4.91	38.00	0.144	0.012676	1.553
300 K, 20 Torr CO in 1 h and evac.	9.54	5.84	1.819	0.002317	4.134
673 K, evac. 2 h	82.70	5.10	18.058	0.015637	36.056
300 K, 20 Torr O_2 in 1 h and evac.	4.85	43.80	0.123	0.014567	1.432
300 K, 20 Torr CO in 1 h and evac.	9.65	5.83	1.843	0.002337	4.182
403 K red., 100 Torr H_2 and evac.	14.30	4.50	3.539	0.002080	6.266
300 K, 20 Torr O_2 in 1 h and evac.	5.30	18.90	0.312	0.006321	2.045
403 K red., 100 Torr H_2 and evac.	14.10	2.70	5.815	0.000205	6.270
300 K, 20 Torr O_2 in 1 h and evac.	7.20	25.40	0.316	0.011991	2.608
403 K red., 100 Torr H_2 and evac.	13.20	2.70	5.444	0.000192	5.870
300 K, 20 Torr O_2 in 1 h and evac.	5.40	23.80	0.253	0.008365	1.987
300 K, 20 Torr CO in 1 h and evac.	5.80	17.90	0.361	0.006496	2.259
673 K evac., 2 h	85.80	5.10	18.734	0.016223	37.407
300 K, 20 Torr O_2 in 1 h and evac.	12.30	21.90	0.625	0.017353	4.611
300 K, 20 Torr CO in 1 h and evac.	20.60	10.20	2.249	0.011535	8.599

(N_B and N_S calculated for $\mu_B = 125$ $cm^2/V \cdot s$ and $\mu_S = 2.5$ $cm^2/V \cdot s$).

for two different mobility negatively charged carriers, and

$$\mu_{meas} = \sigma_{meas}|1/e|\left[\left(-n_B \mu_B^2 + n_S \mu_S^2\right) / \left(n_B \mu_B + n_S \mu_S\right)^2\right] \quad (4)$$

for two opposite-sign carriers, for example a p-type semiconductor with surface trapped electrons. For Eqs. (2)–(4) bulk semiconduction charge carriers have the subscript B and surface vacancy trapped electrons have the subscript S.

As can be seen from the form of Eqs. (3) and (4) for μ_{meas}, two coexisting charge carriers of unequal mobilities will result in measured mobility values that will be in a range between the two actual mobility values for each carrier type. If the difference in mobility values is large, the higher mobility value will dominate, even when the corresponding high-mobility charge carrier is at a relatively low number density. Fig. 1 shows what the measured mobilities would be from Eq. (3) if n-type semiconduction electrons have a mobility of $\mu_B = 100$ $cm^2/V \cdot s$ and surface trapped electrons have mobili-

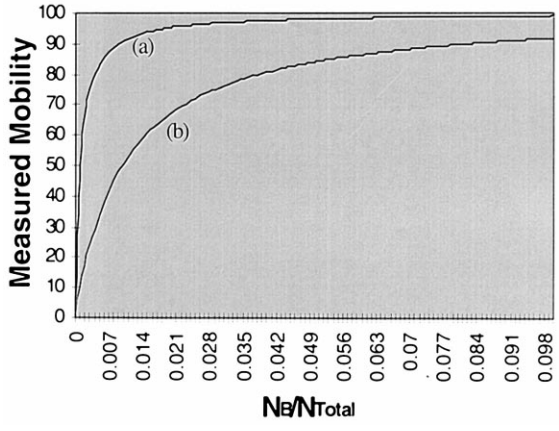

Fig. 1. Measured mobility from Eq. (3).

ties of (a) $\mu_S = 0.1$ cm^2/V·s and (b) $\mu_S = 1$ cm^2/V·s. If Eq. (1) for the single-charge-carrier model is used instead, the resulting N_C values will be significantly lower than the sum of the actual number densities of both charge carriers, $N_{total} = N_B + N_S \gg N_C$. Using the two-charge-carrier model can provide correct values for N_B, N_S, μ_B, and μ_S because the equations used have the proper relationships to the measured mobility and conductivity values.

However, unlike the case for a single charge carrier, we do not have enough equations to find N_B, N_S, μ_B, and μ_S from measured mobilities and conductivities because while there are now two equations, rather than one, there are also four unknowns (N_B, N_S, μ_B, and μ_S), rather than one (N_C). To resolve this problem, values for the mobilities of each of the two charge carrier types needs to be determined separately from the measurements for overall sample μ_{meas} and σ_{meas}. Then the carrier density values can be calculated and checked with other experimental results for quantitative reasonableness.

As can be seen from the μ_{meas} values in Tables 1–6, our measured mobilities range from a low value of 2.5 cm^2/V·s to a high value of 125 cm^2/V·s. This assures $N_B \geq 125$ cm^2/V·s and $N_S \leq 2.5$ cm^2/V·s for the two-charge-carrier model. Using these two μ values for μ_B and μ_S, respectively, would be the most conservative choice. The results of using these μ values in the two-charge-carrier model are shown in Table 6 for the new ZnO powder. Even for these most conservative μ values, the calculated N_S values are consistently higher than the calculated N_C values from the single-charge-carrier model. This means that the single-charge-carrier model can yield grossly underestimated values for low-mobility surface charge carriers when high-mobility bulk, semiconduction charge carriers are present in low concentrations.

3.2. ESR and chemisorption

Both $(V_o^+)^-$ oxygen ion vacancies ($g = 1.96$) and O_2^- ($g = 2.003$) ESR active species were observed on the new ZnO (~ 22 m^2/g) sample. The $(V_o^+)^-$ vacancy concentration reached a high value of 123×10^{15} spins/g after reduction in H_2 at 403 K and was decreased to about one-third of this value following O_2 chemisorption at 300 K. During this latter chemisorption, the O_2^- species reached their maximum value of 716×10^{15} spins/g. These results were qualitatively reproducible during repeated cycling of surface treatments, but exact quantitative reproducibility was not achieved. This quantitative variability in $(V_o^+)^-$ vacancy and O_2^- concentrations is believed due to slow-time-constant changes at, or near, the ZnO surface that are not understood at this time. These changes may be related to a slow decrease in ZnO surface area observed during the surface treatment cycles.

4. Discussion and summary

The high variability in our measured charge carrier mobilities for ZnO powders is not readily explainable by a reasonable physical model for ZnO with a single type of charge carrier. The cycles of surface treatments used would be expected to cause variations in charge carrier number densities, especially for electrons trapped at, or near, the ZnO surface, but not to cause significant variations in mobilities. The use of the two-charge-carrier model resolves this issue by allowing for variations in the number densities, but not the mobilities, of each of the two types of electron charge carriers. Further, most of the variation in charge carrier number density occurs for the low-mobility surface electrons and not for the high-mobility bulk, semiconduction electrons. Because there are two too many unknown quantities for a definitive quantitative analysis using the two-charge-carrier model, some independent means needs to be used to determine two out of the four values for μ_B, μ_S, N_B, and N_S. The measurements of average mobilities provided an upper bound of 2.5 cm^2/V·s for μ_S and a lower bound of 125 cm^2/V·s for μ_B. This suggested the selection of 200 cm^2/V·s for μ_B from previously published mobility values for bulk ZnO semiconductors as a reasonable choice. Any low-mobility charge carriers coexisting in, or on, any of the ZnO samples previously measured would result in lowered measured

values for μ_B. Because of this, the higher value of 200 $cm^2/V \cdot s$ was selected as the most reliable. Because any value between 125 and 200 $cm^2/V \cdot s$ for μ_B will produce comparable results using the two-charge-carrier model, the selection of the higher value for μ_B is also not critical to the results and conclusions of this analysis. Selecting a value for μ_S is more difficult.

The high range value of 0.1 $cm^2/V \cdot s$ for electron mobility in 5 nm ZnO particles [7] corresponds to a electron number density of about 2×10^{19} electrons/g. ZnO(I) powder (with a surface area about the same as the new ZnO powder) had a measured mean particle diameter in the range of 19–32 nm as shown in Table 7. This results in a surface-to-volume ratio about four times lower than that for the 5 nm ZnO particles. The highest N_S value calculated for the new ZnO powder was about 1×10^{18} electrons/g, placing it within an order of magnitude agreement with the $\mu = 0.1$ $cm^2/V \cdot s$ nanoparticle electron number density, assuming that the low-mobility charge carriers are of the same type and are at, or near, the surface of both ZnO materials. Another reason to use the 0.1 $cm^2/V \cdot s$ measured mobility from the 5 nm ZnO study for μ_S is that this nanoparticle mobility value is not affected by any coexisting low-mobility bulk, semiconducting charge carriers — the 5 nm size is too small [7].

Because calculated values for N_S depend greatly on the selected value of μ_S, another quantitative check on the selected μ_S value is the chemisorption of O_2. As pointed out above, ESR measurements of the new ZnO powder give a value of 716×10^{15} spins/g for O_2^- chemisorbed on the new ZnO powder. As shown in Table 5 for the new ZnO powder, the decrease in calculated N_S values under the same surface treatment is about 800×10^{15} electrons/g for the chemisorption of O_2. Assuming that the O_2^- chemisorption to form O_2^- involves the charge-transfer of one surface electron, this is good quantitative agreement. If a lower value of μ_S is used, the N_S and ΔN_S values will be larger and not agree quantitatively with the O_2 chemisorption measurements. And, as can be seen in Table 6, if the higher value of 2.5 $cm^2/V \cdot s$ is used for μ_S the ΔN_S values will be only about 35×10^{15} electrons/g, over 20 times too low.

The suggested chemisorption reactions are

$$2O_2 + (V_o)^{2-} \leftrightarrow \{2O_2^-(V_o^{2+})\}$$

and

$$O_2 + (V_o^+)^- \leftrightarrow \{O_2^-(V_o^{2+})\}$$

The $(V_o^+)^-$ center is observed by ESR after 673 K evacuation and 403 K H_2 reduction, but decreases after O_2 chemisorption. Because the ESR measured change in $(V_o^+)^-$ after O_2 chemisorption is only about 50×10^{15} spins/g, (nearly twenty times too low a spin density to account for the calculated ΔN_S values of about 800×10^{15} electrons/g) the $(V_o)^{2-}$ is suggested as the main surface electron trap on ZnO. Also, because some $(V_o^+)^-$ centers are sometimes observed by ESR after O_2 chemisorption it is suggested that some $(V_o^+)^-$ centers in ZnO are either not able to chemisorb O_2 or that new $(V_o^+)^-$ centers are formed by

$$O_2 + (V_o)^{2-} \leftrightarrow \{O_2^-(V_o^+)^-\}$$

while some previously existing $(V_o^+)^-$ centers are converted to $\{O_2^-(V_o^{2+})\}$. Some $(V_o)^{2-}$ centers may also not chemisorb O_2, but these centers are not directly observable using ESR and no information on their concentrations is available. As shown in Tables 1–6, because some significant calculated values for N_S remain after O_2 chemisorption, this may provide indirect evidence that some $(V_o)^{2-}$ centers, as well as some $(V_o^+)^-$ centers, that have trapped low-mobility conduction electrons, perhaps at internal grain boundaries, may not chemisorb O_2.

Table 7
Average ZnO particle sizes measured by XRD and BET for ZnO(I) and ZnO(II) (Refs. [1,2])

Sample	Treatment	BET (m^2/g)	Particle diameter (nm BET)	Particle diameter (nm XRD)
ZnO(I)	673 K evac., 4 h	32	32	19
ZnO(II)	673 K evac., 1 h	3.4	320	> 80

ESR and chemisorption measurements of ZnO powders thus provide evidence for the validity of calculated N_S values that are consistent with a two-charge-carrier model and that are two-to-three orders of magnitude higher than N_C values calculated from a single-charge carrier model. This determination of much higher surface electron concentrations for ZnO using the two-charge-carrier model should have significant importance to the quantitative understanding of chemisorption and catalysis, especially those materials with low-mobility, bulk, semiconductivity in addition to low-mobility, surface charge carriers.

Acknowledgements

The experimental work reported here was supported by the National Science Foundation (NSF) under Contract No. CBT85-14723, and by the Florida Power and Light Company. Funding for a NSF Equipment Grant (CBT-8505572) is also gratefully acknowledged.

References

[1] B.-K. Na, PhD Thesis, Dept. of Chem. Eng., The Pennsylvania State University, December, 1991.
[2] B.-K. Na, M.A. Vannice, A.B. Walters, Phys. Rev. B 46 (1992) 1266.
[3] B.-K. Na, A.B. Walters, M.A. Vannice, J. Catal. 140 (1993) 585.
[4] C.-C. Liu, PhD Thesis, Dept. of Chem. Eng., The Pennsylvania State University, December, 1991.
[5] C.-C. Liu, B.-K. Na, A.B. Walters, M.A. Vannice, Catal. Lett. 26 (1994) 9.
[6] B.-K. Na, S.L. Kelly, M.A. Vannice, A.B. Walters, Meas. Sci. Technol. 2 (1991) 770.
[7] E.A. Meulencamp, J. Phys. Chem. B 1999 (1999) 7831.